Solid State Sciences 76 (2018) 65–73

Contents lists available at ScienceDirect

Solid State Sciences

journal homepage: www.elsevier.com/locate/ssscie

Increased photocatalytic activity induced by $TiO_2/Pt/SnO_2$ heterostructured films

Glaucio O. Testoni [a, b], Rafael A.C. Amoresi [a, b], Glauco M.M.M. Lustosa [a, b], João P.C. Costa [a], Marcelo V. Nogueira [b], Miguel Ruiz [b], Maria A. Zaghete [a], Leinig A. Perazolli [a, b, *]

[a] Interdisciplinary Laboratory of Electrochemistry and Ceramics, LIEC – Chemistry Institute, São Paulo State University - UNESP, Araraquara, SP, 14800-060, Brazil

[b] Laboratory of Photocatalysis and Microwave Sintering – Chemistry Institute, São Paulo State University - UNESP, Araraquara, SP, 14800-060, Brazil

ARTICLE INFO

Article history:
Received 29 August 2017
Received in revised form
30 November 2017
Accepted 18 December 2017
Available online 21 December 2017

Keywords:
Oxides
Interface
Photocatalysis
Films

ABSTRACT

In this work, a high photocatalytic activity was attained by intercalating a Pt layer between SnO_2 and TiO_2 semiconductors, which yielded a $TiO_2/Pt/SnO_2$ - type heterostructure used in the discoloration of blue methylene (MB) solution. The porous films and platinum layer were obtained by electrophoretic deposition and DC Sputtering, respectively, and were both characterized morphologically and structurally by FE-SEM and XRD. The films with the Pt interlayer were evaluated by photocatalytic activity through exposure to UV light. An increase in efficiency of 22% was obtained for these films compared to those without platinum deposition. Studies on the reutilization of the films pointed out high efficiency and recovery of the photocatalyst, rendering the methodology favorable for the construction of fixed bed photocatalytic reactors. A proposal associated with the mechanism is discussed in this work in terms of the difference in Schottky barrier between the semiconductors and the electrons transfer and trapping cycle. These are fundamental factors for boosting photocatalytic efficiency.

1. Introduction

Environmental pollution has become one of the biggest challenges of our time with its immensurable consequences to living creatures that transcend geographical boundaries. One of the major concerns that need special attention is the imminent shortage of water resources stemming from the accelerated and continued global population growth and the consequent increase in consumption of these limited resources. Considering the areas where water supply fails to meet demand, water reutilization is seen as a suitable alternative for addressing this issue. Among the major pollutants that contribute substantially towards environmental degradation are urban effluents and manufactured chemicals in general, including pesticides, dyes, lubricants, fertilizers, and detergents [1,2]. The need for more efficient yet less costly sustainable technologies for the treatment of effluents and for the control of environmental pollution has essentially become a matter of huge relevance. Synthetic organic dyes with genotoxicity, mutagens and carcinogenic potential have been widely studied because of the unwanted effects of their exposure to biota. Due to their nature, when these dyes are released in effluent water, they are found to be highly detectable, being visible in some cases even in concentrations as low as 1 ppm, causing a marked change in the color of rivers [3,4].

One of the alternative processes employed in water treatment is heterogeneous photocatalysis. This process suitably satisfies defined quality parameters and can clearly be regarded a clean technology, since there is no formation of solid products such as sludge in the biological treatment processes. During their degradation, organic compounds are not only phase transferred but are also destroyed and converted into carbon dioxide, water and inorganic anions; this is a well-known treatment that is based on the generation of OH• radicals [5–7].

The photocatalytic process essentially involves the activation of semiconductors such as TiO_2, SnO_2 [8,9], ZnO [10], among others, through the incidence of sunlight or artificial light. Among these semiconductors, TiO_2 has attracted much attention as a result of its suitable characteristics. Nonetheless, by reason of intrinsic limitations of this semiconductor as far as its photocatalytic performance

* Corresponding author. Interdisciplinary Laboratory of Electrochemistry and Ceramics, LIEC – Chemistry Institute, São Paulo State University - UNESP, Araraquara, SP, 14800-060, Brazil.
E-mail address: leinigp@iq.unesp.br (L.A. Perazolli).

https://doi.org/10.1016/j.solidstatesciences.2017.12.006
1293-2558/

is concerned, much focus has been laid on the study of heterostructures combined with other semiconductors such as SnO_2 [11,12].

The TiO_2 semiconductor is photoactivated through the exposure to UV light with energy equivalent to the bandgap energy, around 3.2 eV. The light excites electrons from the valence band (VB) to the conduction band (CB), leading to the emergence of an electronic hole (h +) in the VB, which, in aqueous medium, promotes the formation of OH• radicals. The photoexcited electron in the CB can be captured by the molecular oxygen adsorbed on the surface of the semiconductor ($O_{2(ads)}$), which is reduced to superoxide radicals ($O_2^{\bullet -}$). Both OH• and $O_2^{\bullet -}$ are responsible for the oxidation of organic compounds. The main goal of conducting photocatalytic studies is to increase the recombination time of e^-/h^+ (see Fig. 1a) [13–15].

TiO_2 and SnO_2 are semiconductors with different bandgap energies. When these semiconductors are obtained as heterostructures and are subjected to light excitation, one notices the occurrence of a charge transfer of the generated photo electrons from TiO_2 for the SnO_2. This leads to an increase in the recombination time, as can be observed in the proposed model shown in Fig. 1b [16,17]. Yaan Cao [17] reported to have produced TiO_2/SnO_2 heterostructured films where they showed that when both the TiO_2 and SnO_2 components of the catalysts are accessible to reactants on the catalyst surface, better improvements are seen in the photocatalytic degradation efficiencies compared to those obtained with TiO_2.

To avoid the recombination of photogenerated charges, some of the methods employed include the formation of composites via the incorporation of some metals into the semiconductor [18,19], commercial oxide mixtures including TiO_2, SnO_2 and Ag_2O [20], $Ti_{1-x}Sn_xO_2$ solid solutions [21], heterojunctions such as $Ag_3VO_4/Fe_3O_4/ZnO$ [22], Cu_2O/Bi_2O_3 [23], SnO_2/TiO_2 [24], and the decoration of semiconductor with metallic nanoparticles [25]. All these methods have been reported to have led to an increase in photocatalytic efficiency by providing a greater charge separation and consequently higher availability of active sites compared to the use of pure TiO_2 [26]. The use of metallic Pt comes with many underlying positive effects including the increase in the separation of electron-hole pair (e^-/h^+) through the trapping of photogenerated electrons and the acceleration of the formation process of superoxide radicals. Other effects worth mentioning are the modification of the adsorption properties of the photocatalyst surface and the improvement in conductivity and interaction between the oxides, favoring the migration of charges onto the surface and thus contributing to the enhancement of the catalytic power of the oxides.

Perazolli et al. [20] published the results of their study on the $SiO_2/Ag/TiO_2$ heterostructure, where they obtained a photoactive power greater than that of P25 – Degussa powder. The authors attributed the high photoactivity attained in their investigation to the formation of a silver metallic interface between the SiO_2 and TiO_2 particles. Other works published in the literature [27,28] have reported the use of metal in the semiconductors directly over the surface where photocatalytic activity takes place. It is worth noting, however, that largely few researchers have reported using metals at the interface region between the two semiconductors. Based on the importance of advanced oxidation processes and heterogeneous photocatalysis in dye inactivation processes, the experiments developed in this work were aimed at obtaining $TiO_2/Pt/SnO_2$ heterostructured film taking into account the relation between TiO_2/Pt and TiO_2/SnO_2 heterostructures for photocatalytic activity in the discoloration of methylene blue dye (MB). A metallic platinum layer was employed in our investigation where it played the role of electrons conductor between the TiO_2 and SnO_2 layers. Clearly, the main purpose of obtaining photocatalytic films with enhanced properties as a result of platinum deposition is to verify the viability of the construction of fixed bed photocatalytic reactors.

2. Experimental procedure

Fig. 2 shows a scheme of heterostructured films investigated in this work. All the films were deposited onto Ti substrate. This substrate was chosen owing to its resistance to oxidation corrosion, high mechanical resistance, and the ability to withstand high temperatures during thermal treatment (up to 1668 °C). Furthermore, the substrate possesses low density (40% of steel density) which facilitates its handling and has chemical affinity with both SnO_2 and TiO_2.

2.1. Semiconductor layers deposition

The films deposition was carried out by the electrophoretic deposition (EPD) technique with each substrate constituted by 1.0 mm of thickness and standard size of 2 × 1 cm. The substrates were sandpapered (sandpaper 1000) in turntable for 5 min at 60 rpm aiming at attaining a homogeneous surface so as to facilitate the adhesion and fixation of the particles. The powders were deposited over an area of 1.5 × 1.0 cm. The EPD process was applied towards the deposition of SnO_2 and TiO_2 particles. This technique has been widely recognized as one of the most versatile mechanisms when it comes to processing particulated materials by virtue of the fact that it entails low cost and speedy working time. In

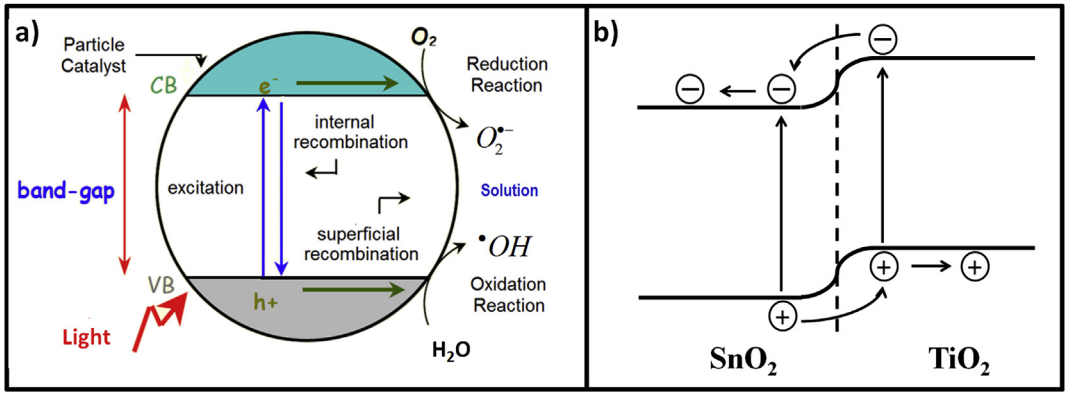

Fig. 1. (a) Activation of a semiconductor by ultraviolet radiation absorption. Adapted from Ziolli et al., 1998 [13], (b) Schematic diagram of the charge-transfer process in the double-layered TiO_2/SnO_2 heterostructured film [17].

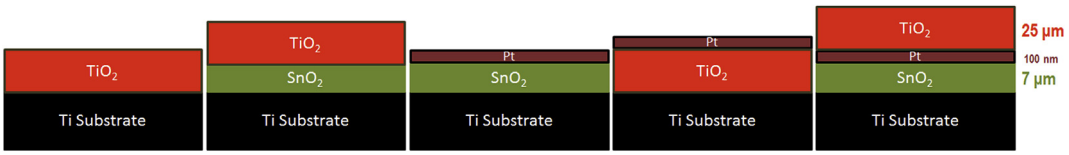

Fig. 2. Scheme of the prepared heterostructured films: TiO_2, TiO_2/SnO_2, SnO_2/Pt, TiO_2/Pt, and $TiO_2/Pt/SnO_2$.

addition, the technique provides one with the ability to adapt deposition according to the shape of the substrate apart from involving simple equipment. As part of the experimental procedure, isopropanol and ethanol were used to prepare suspensions of TiO_2 and SnO_2 particles, respectively. The electrolytic cell system used for deposition was formed by a pair of electrodes (two Ti substrates), a glass beaker and alcoholic suspension (25 mL) containing the oxide, as shown in Fig. 3. The Ti substrates were placed at a distance of 20 mm and immersed in the solution containing the particles. Through the use of a high voltage source (Fug - High voltage power supply-series HCP 350–6500), a voltage of 1.5 kV was applied during defined periods of time for each film type as specified below. One will note that the current indication is in the range of 2.0 mA and the oxides were deposited on negative electrode (cathode).

The first goal was to determine the deposition time of SnO_2 particles so as to obtain a film with homogeneous thickness and with full covering of the substrate surface. For the deposition of SnO_2 particles by EPD, a suspension was prepared using 20 mL of ethanol and 10 mg of commercial tin dioxide powder (CF Cesbra with 99.9% purity and an average particle diameter of 0.15 µm) with the addition of 10 mg of polymethylmethacrylate (PMMA) to increase the surface charge of the particles and improve deposition. The suspension was homogenized in an ultrasound for 5 min. The deposition process was tested by applying 1.5 kV for 5,10,15 and 20 min. The film obtained at lower times did not show the full covering of the substrate. By contrast, the film obtained when the voltage was applied for 20 min exhibited higher deposition of particles, resulting in a greater covering of the substrate.

For the deposition of TiO_2 layers, deposition tests were performed for 5, 10, 15 and 20 min under 1.5 kV with 10 mg of commercial TiO_2 powder (Vetec, 98% of purity, average particle diameter: 100 nm) and 20 mL of isopropyl alcohol. The solution was subsequently subjected to ultrasound for 5 min to enable the particles homogenization. An adjustment was made on the electrodes with a magnet as shown in Fig. 3, where one can observe the appearance of a magnetic field in the system, which contributed towards enhancing the deposition of the particles. This magnetic coupling with an adaptation of the cell electrodes was found to be efficient; this was key to obtaining a homogeneous film with good adhesion to the substrate in less time. The films obtained after 15 and 20 min of deposition exhibited a surface with cracks as a result of the larger deposition time of the particles. On the other hand, for the film deposited for 5 min, the time was not sufficient enough to enable the covering of the substrate surface. As such, 10 min was chosen as the suitable deposition time for obtaining the TiO_2 layer.

2.2. Pt deposition and preparation of the heterostructured film

Following the deposition of the layers, both TiO_2 and SnO_2 films were heat treated at 450 °C/60 min using microwave oven. The platinum layer was deposited by DC Sputtering on the sample surface after the deposition and heat treatment of the SnO_2 particles layer. To this end, we employed the Sputter Equipment Denton Vacuum DV - 502A coupled to an energy source Sorensen DCS 600–1.7, under a voltage of 350 V, which was applied for 10 min with a current of 0.07 A. The deposition time of the platinum layer was set at 10 min after conducting tests to obtain a homogeneous surface and low surface roughness.

2.3. Characterization

XRD (X-ray diffraction) using Rigaku equipment RINT2000 model for the analysis of crystalline phase was carried out with experimental conditions ranging from 20° to 80° with an increment of $\Delta 2\theta = 0.02°$ and copper radiation, 40 kV and 20 mA. FE-SEM (Field emission scanning electron microscopy) - JEOL 7500F model, was used for the evaluation of the films morphology.

2.4. Photocatalytic tests

The photocatalysis experiments were carried out in a fixed bed reactor using a high pressure mercury lamp of 80 W in quartz tube maintained at controlled temperature (20 °C). 300 mL aqueous solution of the methylene blue dye (MB) was used at a concentration of 5.0×10^{-6} mol L^{-1} with exposure to UV radiation for

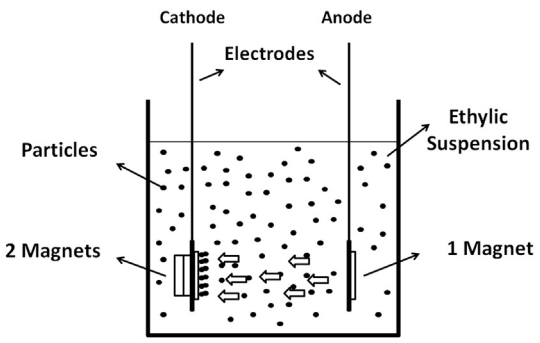

Fig. 3. Electrophoretic deposition system developed by the authors [11].

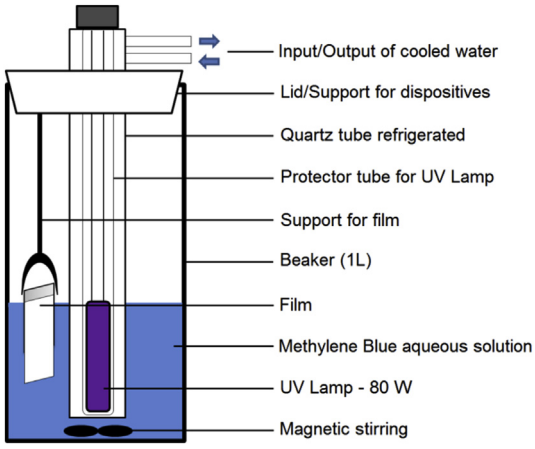

Fig. 4. Reactor for photocatalytic experiments.

120 min. The films were fixed and immersed in solution, with the films surface facing the UV- lamp (Fig. 4). During the entire process, the system was kept at 20 °C, with magnetic stirring and bubbling atmospheric air. Aliquots were taken over the periods of 0, 5, 10, 15, 30, 45, 60, 90 and 120 min for analysis using UV–Vis scanning spectrophotometer (Femto Cirrus 80 PR) aiming at obtaining the absorption spectra and the subsequent calculation of the discoloration percentage of the MB aqueous solution [29,30]. To ascertain the dye concentration from a given period to another, linear correlation was calculated in terms of the dye discoloration and the absorbance at $\lambda_m = 670$ nm.

The calculation method regarding the discoloration was based on equation (1) below:

$$Disc = \left(\frac{1 - A_{670(t)}}{A_{670(0)}}\right) \times 100 \quad (1)$$

Where A_{670} is the absorbance at $\lambda_m = 670$ nm.

2.5. Films cleaning

Following the use of the films in the photocatalytic process, reutilization tests were conducted where the films were made to undergo cleaning cycles. These cycles involve the immersion of the films into a 20 mL ethyl solution containing 1 M of NaOH for 5 min prior to washing them with distilled water. The washed film was subsequently employed towards the photodiscoloration of a new MB aqueous solution.

3. Results and discussion

3.1. Films morphology and structure

TiO_2 and SnO_2 films were characterized structurally by XRD as depicted in Fig. 5. Fig. 5a shows the diffractogram for SnO_2 film indicating the rutile crystalline phase (JCPDS Card No. 41–1445). The peaks observed show the characteristic crystallographic planes essentially typical of polycrystalline samples. Furthermore, some other peaks that can be identified appearing with less intensity are attributed to titanium substrate. Fig. 5b shows XRD analysis of the TiO_2 film obtained. The peaks observed in the diffractogram indicate the presence of the anatase phase (JCPDS Card No. 21–1272).

Fig. 6 shows the SEM images for the TiO_2 and SnO_2 films. For both films, the images indicate uniformity, with good particles dispersion and thickness of about 7 μm and 25 μm for SnO_2 and TiO_2 films respectively. The microscopies also demonstrate that the films exhibit porous morphology which can be seen to be less dense compared to the films obtained via other methods. The result can be attributed to the low temperature of the thermal treatment (at 450 °C). Essentially, the fact that relatively lesser energy is consumed during the heat treatment in addition to the lower temperature involved compared to that of the change of TiO_2 phase (anatase - rutile) make the methodology comparatively more advantageous. Based on the aforementioned conditions for obtaining the films, the remaining heterostructures presented in Fig. 2 were constructed. The interface is shown in Fig. 6c. In this figure, one can observe the region of contact between TiO_2/Pt/SnO_2, the particle size between 50 and 150 nm and the junction between the semiconductors and the metal. Fig. 6d illustrates the microstructure of the TiO_2 film surface showing the neck formation between the particles. This is indicative of the fact that the heat treatment was enough to achieve the initial sintering stage of the particles in the TiO_2 film.

3.2. Photocatalytic activity

Photocatalytic tests were performed in order to assess the photoactivity of each of the materials obtained. The results derived from the discoloration of the MB aqueous solution are illustrated in Fig. 7a. The degradation curves point to a first order kinetic behavior as shown in Fig. 7b of *Ln(C)* versus *t*. The kinetic process is described by equation (2) below [29,30]:

$$Ln(C) = Ln(C_0) - Kt \quad (2)$$

In this equation, C stands for MB dye relative to concentration at time t, C_0 being the initial concentration, and K the first order constant rate. The results presented in Table 1 indicate a correlation coefficient (R^2) in the range of 0.92–0.98 for all the curves, confirming the first order model for reaction. In addition, these same results reveal that TiO_2 films and the TiO_2/SnO_2 or TiO_2/Pt heterostructures exhibit similar patterns of behavior regarding photocatalytic activity with a slight increase in degradation for TiO_2 films. These similar outcomes observed in the heterostructures can be attributed to the low interaction between either the interface of the semiconductors TiO_2/SnO_2 or that of TiO_2/Pt. The kinetic constant is seen to follow the same pattern, being greater for the TiO_2 film compared to that of the TiO_2/SnO_2 and TiO_2/Pt heterostructures. With results similar to those exhibited by photolysis, the SnO_2/Pt film was found to present low photoactivity. Considering the effective photoabsorption of the materials through the lamp used in the experimental procedure, our data are strictly in line with the

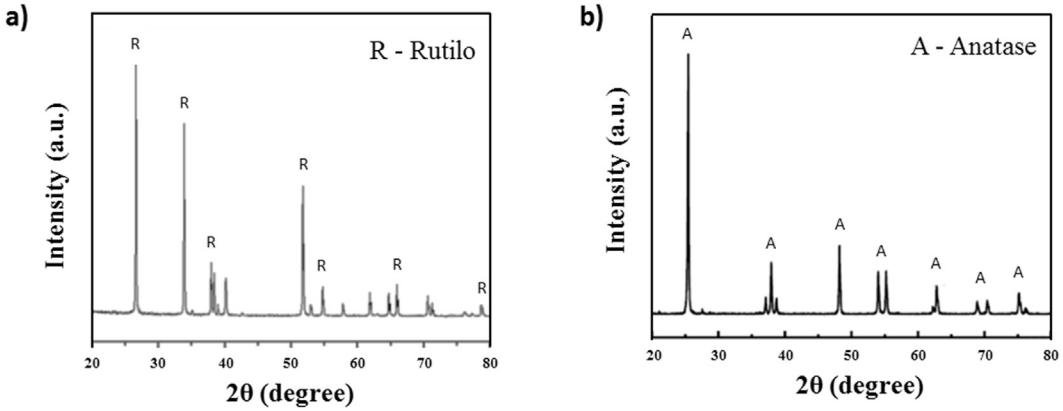

Fig. 5. XRD patterns of a) SnO_2 and b) TiO_2 films.

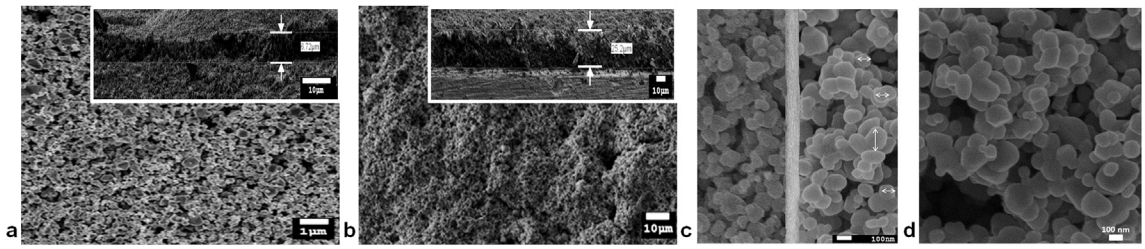

Fig. 6. FE-SEM images of a) surface of SnO_2 film deposited at 20 min, b) surface of TiO_2 film deposited at 10 min (inset: cross section of each film), c) interface of the heterostructure: SnO_2 at the left, Pt in the middle, and TiO_2 at the right, and d) TiO_2 film with deposition time of 10 min and surface detail.

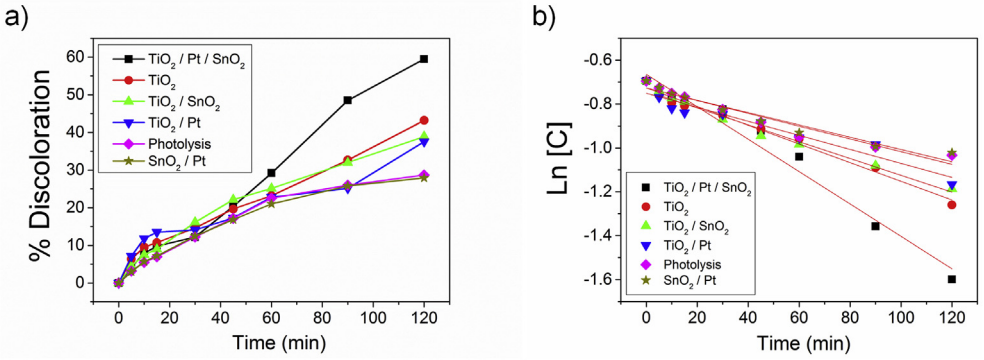

Fig. 7. (a) Discoloration of MB aqueous solution for the films prepared and under investigation: $TiO_2/Pt/SnO_2$, TiO_2, TiO_2/SnO_2, TiO_2/Pt, Photolysis and SnO_2/Pt. (b) Graph of kinetic constant versus time.

Table 1
Discoloration percentage and kinetic constant model for TiO_2 film, heterostructured films, and photolysis.

Film	% discoloration	$\lvert Ln[C_0]\rvert$	$[C_0]$ mg L^{-1}	K (min^{-1})	R^2
$TiO_2/Pt/SnO_2$	59.5	0.66	0.52	7.4×10^{-3}	0.97
TiO_2	43.2	0.73	0.48	4.3×10^{-3}	0.98
TiO_2/SnO_2	38.9	0.74	0.48	3.8×10^{-3}	0.98
TiO_2/Pt	37.5	0.75	0.47	3.2×10^{-3}	0.92
Photolysis	28.7	0.73	0.48	2.9×10^{-3}	0.94
SnO_2/Pt	27.9	0.73	0.48	2.8×10^{-3}	0.95

reports published in the literature concerning the heterostructures [17,25].

With regard to the $TiO_2/Pt/SnO_2$ heterostructure, the use of Pt interlayer contributed towards improving the photocatalysis efficiency to over 59.5% at 120 min, as observed in Table 1. This material presented the highest discoloration percentage and greatest constant K. As shown in Fig. 8, the kinetic behavior of these materials relative to photocatalytic activity is found to be different. In Fig. 8a, one can observe the pattern of behavior of TiO_2 film where the discoloration velocity relative to time is seen as a typical curve of the photocatalytic activity of titanium dioxide. For the TiO_2/SnO_2 and TiO_2/Pt heterostructures (Fig. 8b–c), there is a slight tendency of a rise in velocity in the regions of 40 (Fig. 8b) and 60 min (Fig. 8c) of photocatalytic reaction. One will notice, nonetheless, that the reaction curve as a whole is similar to the curve attributed to the photocatalytic reaction of pure TiO_2 (Fig. 8a). This can be explained by the fact that the TiO_2 and SnO_2 layers in the heterostructured films were only able to reach the initial stages of sintering (Fig. 6-d) with coalescence between the particles.

Interestingly, a distinct behavior is observed for the $TiO_2/Pt/SnO_2$ heterostructured film where the velocity is found to increase significantly following 30 min of reaction (Fig. 8d). Based on our analysis, this behavior is attributed to the Pt layer. By general understanding [10,31], upon the occurrence of an effective contact between TiO_2/SnO_2, it is believed that the mechanism responsible for photocatalytic activity takes place through the oxidation of the dye by holes (h^+) generated in the photocatalyst. This is so because the electrons (e^-) is thought to be removed from the surface and consumed by the reduction of O_2 at the interface of the SnO_2 film. In our investigation, we expected to see an improvement in photocatalytic activity in the TiO_2/SnO_2 heterostructure [17]. Nevertheless, the films obtained by EPD presented low contact adhesion between the layers. This is as a result of the low thermal energy supplied during the heat treatment (450 °C), which, consequently, led to a decline in efficient interaction between the layers of the semiconductors only. In the case of the heterostructured $TiO_2/Pt/SnO_2$, electronic contact is thought to be promoted upon the insertion of the platinum layer between the two semiconductors, as shown in Fig. 6c. It is this synergy that acts as an efficient vehicle of interaction between the two semiconductors. In this system, the manner in which the heterojunction was constructed ($TiO_2/Pt/SnO_2$) played a pivotal role in aiding the electrons transfer. The insertion of the platinum layer at the TiO_2/SnO_2 interface made the transfer of electrons possible from TiO_2 to SnO_2. In this case, the metallic layer promotes contact between the layers of the semiconductors. As can be observed in the Pt/TiO_2 junction from the scheme proposed in Fig. 9, upon subjecting the TiO_2 surface to irradiation using photons, the electrons are found to be excited to the conduction band where they subsequently move towards the Pt layer. The semiconductor/metal interface forms the Schottky barrier (ϕ_b), which depends on the metal/semiconductor combination, leading to electronic conduction. Theoretically, the Schottky barrier seen between Pt/SnO_2 is smaller than that of Pt/TiO_2, as can be observed in the following equations (3)–(5) and calculations:

$$\Phi_b = \Phi_m - \chi \tag{3}$$

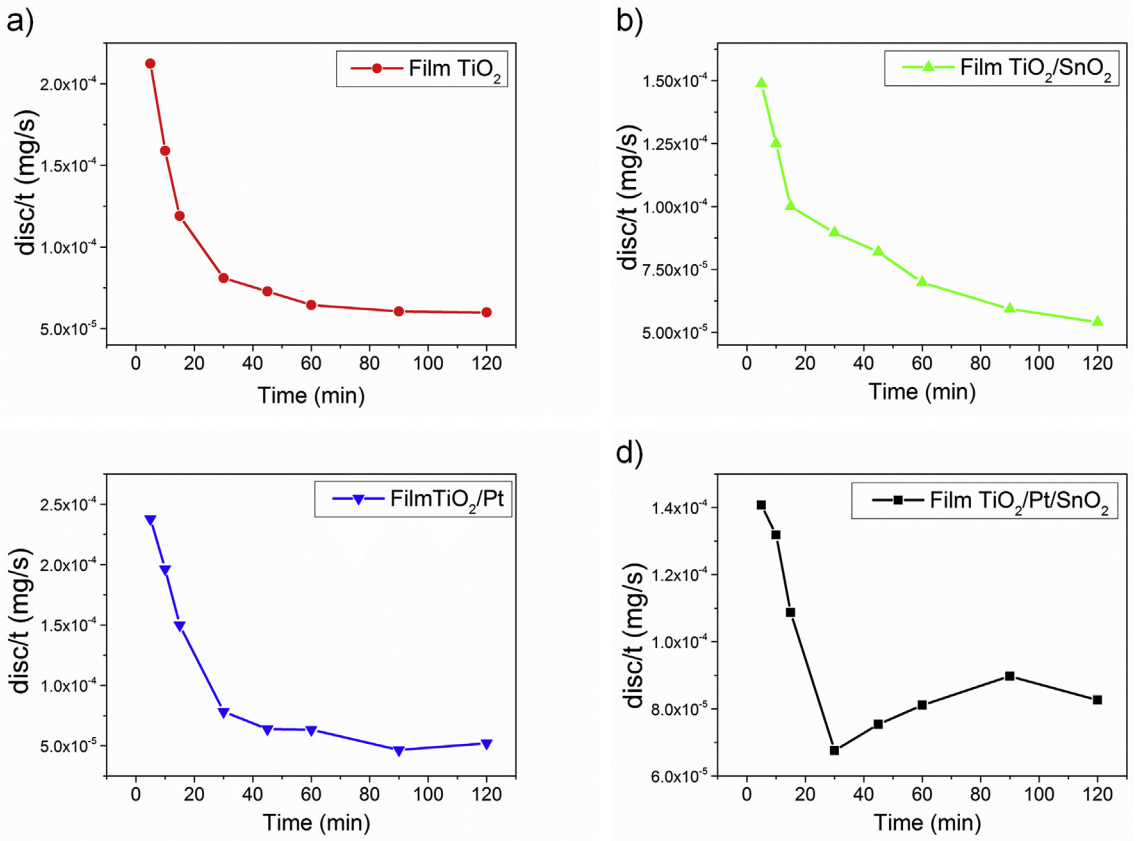

Fig. 8. Velocity of discoloration in relation to time for a) TiO_2 film and the heterostructured films including b) TiO_2/SnO_2, c) TiO_2/Pt and d) $TiO_2/Pt/SnO_2$.

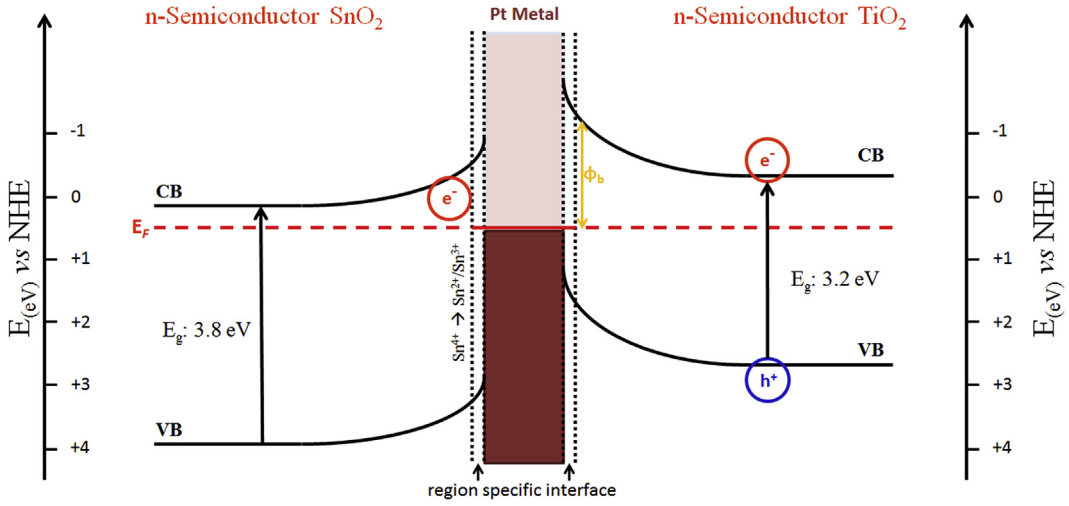

Fig. 9. Photocatalytic activity scheme for the $TiO_2/Pt/SnO_2$ heterostructure (Image produced by the authors and values taken from Hattori et al., 2001 [31].).

$$\Phi_{b\ SnO2} = 5.65 - 4.1 = 1.55 \quad (4)$$

$$\Phi_{b\ TiO2} = 5.65 - 2.2 = 3.45 \quad (5)$$

Here, Φ_b represents the Schottky barrier, $\Phi_m$is the work function of metal and χ the electronic affinity of the semiconductor [32,33]. The platinum layer will, thus, be capable of trapping electrons coming from the surface of TiO_2. The Pt/SnO_2 interface, with a smaller Schottky barrier, will tend to attract electrons that have been trapped by the Pt layer [17]. Hence, one will note that both the electrons and holes generally act in the degradation of the dye, causing a saturation and decline in the photocatalytic activity. The presence of the semiconductor/Pt interface works as a way to transfer of electron between the semiconductors, avoiding the recombination of electron-holes while prolonging the photocatalytic activity. This proposed mechanism of photodegradation resembles the one reported by Huang et al. [34–36]. In their

published work, the authors showed that the transfer of charges in the interface region results in the accumulation of photogenerated electrons in the conduction band. Based on their study, the electrons are completely transformed into $^{\bullet}O_2^-$ through the reduction of O_2, and thus act as reactive species in the photocatalytic degradation. Other hypothesis is that a second mechanism may prompt the movement of the electrons from the metal to the semiconductor [26], causing the reduction of tin oxide at the interface, as described in equations (6) and (7):

$$Sn^{4+} + 1e^- \rightarrow Sn^{3+} \quad (6)$$

$$Sn^{4+} + 2e^- \rightarrow Sn^{2+} \quad (7)$$

Thus, the use of platinum favors the transfer of charges in the interface region, slowing down the electron-hole recombination while possibly contributing towards tin reduction. Basically, it plays a key role in the capture of electrons coming from the surface, thereby promoting a continuous process of electron-hole generation.

3.3. Photocatalyst robustness: reutilization and variation of photocatalysis area

A series of new tests were carried out with new MB aqueous solutions with the aim of proving the feasibility of the reuse of the $TiO_2/Pt/SnO_2$ film. By subjecting it to this whole process, the film reached a point of saturation, which, thus, led to the reduction of its efficiency. A crucial point worth mentioning regarding the reutilization of films is that their efficiency is not constant. This fact is attributed to the poisoning of the surface, which makes it necessary to interrupt the discoloration process while readjusting the film for subsequent reuse. In doing so, a cleaning cycle is completed. Fig. 10 shows the results of efficiency according to the experiment time for the film reutilization and the use of two films with and without cleaning mechanism.

The use of a single film of $TiO_2/Pt/SnO_2$, for the first time, yielded 59.5% discoloration (Fig. 7) with kinetic constant (K) of 7.4×10^{-3} min^{-1}. After making the needed adjustments for the film reutilization process, the rate of discoloration obtained was 57.4% with K of 7.1×10^{-3} min^{-1}. These results proved satisfactory since they are related to the films reutilization. Besides eliminating the powder recovery step, reused films were found to ensure greater flexibility for the manufacture of fixed bed reactors. With adequate and periodic cleaning steps, it is not necessary to employ other films at a short period of time, thereby reducing the costs of the process.

Considering the premise that an increase in the number of films leads to a higher discoloration rate, tests were conducted regarding the simultaneous use of two $TiO_2/Pt/SnO_2$-films for the discoloration of MB aqueous solution. A comparative analysis was made on the efficiencies of the photodiscoloration of MB aqueous solution; this comparison can be found depicted in Fig. 10 and Table 2. The use of an additional film in the reactor was seen to favor the discoloration rate. An efficiency rate of 76.0% and K of 1.1×10^{-2} min^{-1} were obtained after 120 min of treatment. The kinetic constant of 1.1×10^{-2} min^{-1} is, indeed, the highest value obtained for experiments with films in this work. The value obtained for the efficiency rate represents an increase of 16.5% in photocatalytic efficiency compared to the use of a single film. Based on these results, we believe that a gradual increase of films in the reactor results in greater efficiency of photocatalytic activity. Studies are being conducted by our research group aiming at finding out the relation between the area of the films and the comprehensive nature of photocatalysis when it comes to the degradation of dyes. At this juncture, it is worth pointing out the merit associated with the use of cleaning cycles. As indicated by our results, the reuse of the two films without subjecting them to cleaning yielded a discoloration of 61.5% and kinetic constant (k) of 7.6×10^{-3} min^{-1}. The cleaning cycle enabled us to achieve 71.4% of efficiency while contributing towards improving the kinetic constant (k) to 1.0×10^{-2} min^{-1}. The efficiency rate obtained here represents an increase of ~10.0% in discoloration compared to the non-cleaning process. This, undoubtedly, demonstrates the importance of the cleaning step in practical purposes. Considering that the films have a limited useful life and degree of saturation of active sites coupled with the fact that the sub-products of discoloration are the main cause of poisoning, the process involves the employment of cleaning cycles/stages with appropriate NaOH solution. This ensures the restoration of the films efficiency instead of solely relying on the use of new films.

4. Conclusion

This work reported the successful development of a film constituted by an interlayer of metallic Pt between layers of TiO_2 and SnO_2 commercial oxides on a titanium metal substrate through the use of sputtering and electrophoresis deposition techniques. The heterostructured films exhibited photocatalytic activity for the discoloration of methylene blue aqueous solutions. The use of a Pt interlayer raised the efficiency to 60% compared to that of 37.6% for TiO_2/SnO_2 film. The use of a single film for the discoloration of MB aqueous solution showed an efficiency of 60%, which was subsequently elevated to 76% upon employing two simultaneous films. The use of two or more films proved to be essentially advantageous

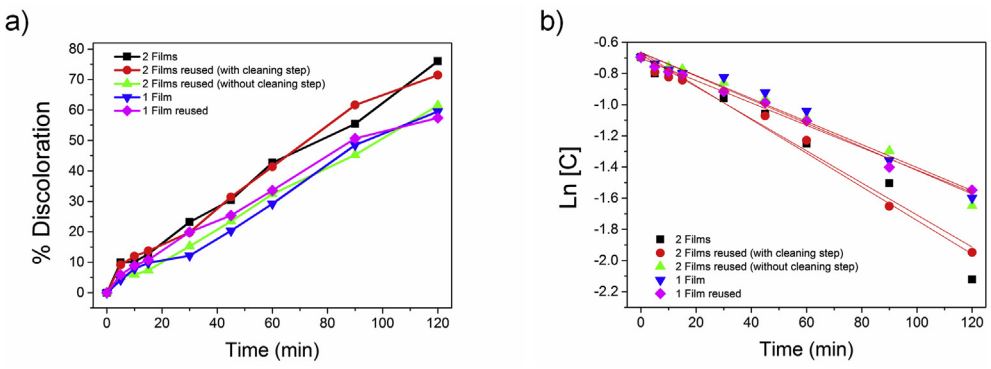

Fig. 10. a) Discoloration of MB aqueous solution for $TiO_2/Pt/SnO_2$ heterostructured films: Two films, two films reused (with and without cleaning step), one film and one film reused with cleaning step, (b) Graph of kinetic constant of photodiscoloration.

Table 2
Discoloration percentage and kinetic constant model for reused films and variation of the photocatalytic area.

Film	% discoloration	ıLn[C_0]ı	[C_0] mg L^{-1}	K (min^{-1})	R^2
Two films	76.0	0.66	0.52	1.1×10^{-2}	0.96
Two reused films (with cleaning step)	71.4	0.68	0.51	1.0×10^{-2}	0.98
Two reused films (without cleaning step)	61.5	0.67	0.51	7.6×10^{-3}	0.98
One film	59.5	0.66	0.52	7.4×10^{-3}	0.97
One reused film	57.4	0.70	0.50	7.1×10^{-3}	0.99

once it contributed towards obtaining a higher percentage of discoloration at a relatively shorter period of time. The reuse of the films was rendered possible through the addition of a cleaning stage between cycles of discoloration/degradation. The cleaning cycles promoted a remarkable efficiency rate of the films similar to the rate they exhibited when they were initially used. The use of platinum layer between the semiconductors helped to optimize the photocatalytic process. Furthermore, the methodology applied in this study with respect to the films reutilization is clearly favorable for the construction of fixed bed reactors.

Acknowledgements

The authors would like to express their sincerest gratitude and indebtedness to the LMA-IQ for providing the FEG-SEM facilities, and to the Brazilian research funding agencies CNPq and CEPID/CDMF-FAPESP (process no. 2013/07296-2) for the financial support granted during the course of this research project.

References

[1] N. Li, Y. Hu, Y.-Z. Lu, R.J. Zeng, G.-P. Sheng, Multiple response optimization of the coagulation process for upgrading the quality of effluent from municipal wastewater treatment plant, Sci. Rep. 6 (2016) 26115, https://doi.org/10.1038/srep26115.
[2] M. Osman, Waste water treatment in chemical industries: the concept and current technologies, J. Waste Water Treat. Anal. 5 (2014) 1–12, https://doi.org/10.4172/2157-7587.1000164.
[3] S.H.S. Chan, T.Y. Wu, J.C. Juan, C.Y. Teh, Recent developments of metal oxide semiconductors as photocatalysts in advanced oxidation processes (AOPs) for treatment of dye waste-water, J. Chem. Technol. Biotechnol. 86 (2011) 1130–1158, https://doi.org/10.1002/jctb.2636.
[4] H. Langhals, Color chemistry. Synthesis, properties and applications of organic dyes and pigments. 3rd revised edition. By Heinrich Zollinger, Angew. Chem. Int. Ed. 43 (2004) 5291–5292, https://doi.org/10.1002/anie.200385122.
[5] B. Yang, J. Wang, C. Jiang, J. Li, G. Yu, S. Deng, S. Lu, P. Zhang, C. Zhu, Q. Zhuo, Electrochemical mineralization of perfluorooctane sulfonate by novel F and Sb co-doped Ti/SnO2 electrode containing Sn-Sb interlayer, Chem. Eng. J. 316 (2017) 296–304, https://doi.org/10.1016/j.cej.2017.01.105.
[6] Y. Peng, K.K. Wang, T. Liu, J. Xu, B.G. Xu, Synthesis of one-dimensional Bi2O3-Bi2O2.33 heterojunctions with high interface quality for enhanced visible light photocatalysis in degradation of high-concentration phenol and MO dyes, Appl. Catal. B Environ. 203 (2017) 946–954, https://doi.org/10.1016/j.apcatb.2016.11.011.
[7] A.L. Pruden, D.F. Ollis, Photoassisted heterogeneous catalysis: the degradation of trichloroethylene in water, J. Catal. 82 (1983) 404–417, https://doi.org/10.1016/0021-9517(83)90207-5.
[8] M.F. Abdel-Messih, M.A. Ahmed, A.S. El-Sayed, Photocatalytic decolorization of Rhodamine B dye using novel mesoporous SnO2-TiO2 nano mixed oxides prepared by sol-gel method, J. Photochem. Photobiol. A Chem. 260 (2013) 1–8, https://doi.org/10.1016/j.jphotochem.2013.03.011.
[9] T.H. Le, Q.D. Truong, T. Kimura, H. Li, C. Guo, S. Yin, T. Sato, Y.C. Ling, Construction of 3D hierarchical SnO2 microspheres from porous nanosheets towards NO decomposition, Solid State Sci. 15 (2013) 29–35, https://doi.org/10.1016/j.solidstatesciences.2012.09.004.
[10] S.M. Lam, J.C. Sin, A.Z. Abdullah, A.R. Mohamed, Degradation of wastewaters containing organic dyes photocatalysed by zinc oxide: a review, Desalin. Water Treat. 41 (2012) 131–169, https://doi.org/10.1080/19443994.2012.664698.
[11] G.M.M.M. Lustosa, J.P. de Campos da Costa, L.A. Perazolli, B.D. Stojanovic, M.A. Zaghete, Potential barrier of (Zn,Nb)SnO2-Films induced by microwave thermal diffusion of Cr3+ for low-voltage varistor, J. Am. Ceram. Soc. 99 (2016) 152–157, https://doi.org/10.1111/jace.13924.
[12] A. Hattori, Y. Tokihisa, H. Tada, S. Ito, Acceleration of oxidations and retardation of reductions in photocatalysis of a TiO_2/SnO_2 bilayer-type catalyst, J. Electrochem. Soc. 147 (2000) 2279–2283, https://doi.org/10.1149/1.1393521.
[13] R.L. Ziolli, W.F. Jardim, Mecanismo de fotodegradação de compostos orgânicos catalisada por TiO_2, Quím. Nova 21 (1998) 319–325, https://doi.org/10.1590/S0100-40421998000300013.
[14] A. Samokhvalov, Hydrogen by photocatalysis with nitrogen codoped titanium dioxide, Renew. Sustain. Energy Rev. 72 (2017) 981–1000, https://doi.org/10.1016/j.rser.2017.01.024.
[15] A.L. Linsebigler, G. Lu, J.T. Yates, Photocatalysis on TiO2 surfaces: principles, mechanisms, and selected results, Chem. Rev. 95 (1995) 735–758, https://doi.org/10.1021/cr00035a013.
[16] B. Levy, W. Liu, S.E. Gilbert, Directed photocurrents in nanostructured TiO2/SnO2 heterojunction diodes, J. Phys. Chem. B 101 (1997) 1810–1816, https://doi.org/10.1021/jp962105n.
[17] Y. Cao, X. Zhang, W. Yang, H. Du, Y. Bai, T. Li, J. Yao, A bicomponent TiO2/SnO2 particulate film for photocatalysis, Chem. Mater. 12 (2000) 3445–3448, https://doi.org/10.1021/cm0004432.
[18] H.W. Wang, H.C. Lin, C.H. Kuo, Y.L. Cheng, Y.C. Yeh, Synthesis and photocatalysis of mesoporous anatase TiO2 powders incorporated Ag nanoparticles, J. Phys. Chem. Solid. 69 (2008) 633–636, https://doi.org/10.1016/j.jpcs.2007.07.052.
[19] X. Yu, F. Liu, J. Bi, B. Wang, S. Yang, Improving the plasmonic efficiency of the Au nanorod-semiconductor photocatalysis toward water reduction by constructing a unique hot-dog nanostructure, Nano Energy 33 (2017) 469–475, https://doi.org/10.1016/j.nanoen.2017.02.006.
[20] L. Perazolli, G.F. Pegler, M.R.A. Silva, R.A.F. Ingino, J.A. Varela, High activity photocatalyst powder formed by three ceramic oxides, Adv. Sci. Technol. 65 (2010) 184–193, https://doi.org/10.4028/www.scientific.net/AST.65.184.
[21] J. Lin, J.C. Yu, D. Lo, S.K. Lam, Photocatalytic activity of rutile Ti1-xSnxO2 solid solutions, J. Catal. 183 (1999) 368–372, https://doi.org/10.1021/cm902970u.
[22] M. Shekofteh-Gohari, A. Habibi-Yangjeh, Combination of $CoWO_4$and $Ag_3VO_4$with Fe_3O_4/ZnO nanocomposites: magnetic photocatalysts with enhanced activity through p-n-n heterojunctions under visible light, Solid State Sci. 74 (2017) 24–36, https://doi.org/10.1016/j.solidstatesciences.2017.10.001.
[23] M. Miodynska, B. Bajorowicz, W. Lisowski, T. Klimczuk, J. Winiarski, A. Zaleska-medynska, J. Nadolna, Preparation and photocatalytic properties of $BaZrO_3$ and $SrZrO_3$ modified with Cu_2O/Bi_2O_3 quantum dots, 74 (2017) 13–23.
[24] K. Vinodgopal, I. Bedja, P.V. Kamat, Nanostructured semiconductor films for photocatalysis. Photoelectrochemical behavior of SnO_2/TiO_2 composite systems and its role in photocatalytic degradation of a textile azo dye, Chem. Mater. 8 (1996) 2180–2187, https://doi.org/10.1021/cm950425y.
[25] J. Bian, Y. Qu, R. Fazal, X. Li, N. Sun, L. Jing, Accepting excited high-energy-level electrons and catalyzing H_2 evolution of dual-functional Ag-TiO_2 modifier for promoting visible-light photocatalytic activities of nanosized oxides, J. Phys. Chem. C 120 (2016) 11831–11836, https://doi.org/10.1021/acs.jpcc.6b03664.
[26] H. Zhang, G. Chen, D.W. Bahnemann, Photoelectrocatalytic materials for environmental applications, J. Mater. Chem. 19 (2009) 5089, https://doi.org/10.1039/b821991e.
[27] S. Xun, Z. Zhang, T. Wang, D. Jiang, H. Li, Synthesis of novel metal nanoparticles/$SnNb_2O_6$ nanosheets plasmonic nanocomposite photocatalysts with enhanced visible-light photocatalytic activity and mechanism insight, J. Alloys Compd. 685 (2016) 647–655, https://doi.org/10.1016/j.jallcom.2016.05.260.
[28] K. Ji, H. Dai, J. Deng, H. Zang, H. Arandiyan, S. Xie, H. Yang, 3DOM $BiVO_4$ supported silver bromide and noble metals: high-performance photocatalysts for the visible-light-driven degradation of 4-chlorophenol, Appl. Catal. B Environ. 168–169 (2015) 274–282, https://doi.org/10.1016/j.apcatb.2014.12.045.
[29] C.H. Kwon, H. Shin, J.H. Kim, W.S. Choi, K.H. Yoon, Degradation of methylene blue via photocatalysis of titanium dioxide, Mater. Chem. Phys. 86 (2004) 78–82, https://doi.org/10.1016/j.matchemphys.2004.02.024.
[30] B. Mounir, M.N. Pons, O. Zahraa, A. Yaacoubi, A. Benhammou, Discoloration of a red cationic dye by supported TiO2 photocatalysis, J. Hazard Mater. 148 (2007) 513–520, https://doi.org/10.1016/j.jhazmat.2007.03.010.
[31] A. Hattori, Y. Tokihisa, H. Tada, N. Tohge, S. Ito, K. Hongo, R. Shiratsuchi, G. Nogami, Patterning effect of a sol-gel TiO_2 overlayer on the photocatalytic activity of a TiO2/SnO2 bilayer-type photocatalyst, J. Sol. Gel Sci. Technol. 22 (2001) 53–61, https://doi.org/10.1023/A:1011212303299.
[32] H.B. Michaelson, The work function of the elements and its periodicity, J. Appl. Phys. 48 (1977) 4729–4733, https://doi.org/10.1063/1.323539.
[33] J. Robertson, Band offsets, Schottky barrier heights, and their effects on electronic devices, J. Vac. Sci. Technol. A Vac. Surfaces Film 31 (2013) 50821,

https://doi.org/10.1116/1.4818426.
[34] H. Huang, X. Han, X. Li, S. Wang, P.K. Chu, Y. Zhang, Fabrication of multiple heterojunctions with tunable visible-light-active photocatalytic reactivity in BiOBr-BiOI full-range composites based on microstructure modulation and band structures, ACS Appl. Mater. Interfaces 7 (2015) 482–492, https://doi.org/10.1021/am5065409.
[35] H. Huang, K. Xiao, Y. He, T. Zhang, F. Dong, X. Du, Y. Zhang, In situ assembly of BiOI@Bi12O17Cl2 p-n junction: charge induced unique front-lateral surfaces coupling heterostructure with high exposure of BiOI {001} active facets for robust and nonselective photocatalysis, Appl. Catal. B Environ. 199 (2016) 75–86, https://doi.org/10.1016/j.apcatb.2016.06.020.
[36] H. Huang, S. Tu, C. Zeng, T. Zhang, A.H. Reshak, Y. Zhang, Macroscopic polarization enhancement promoting photo- and piezoelectric-induced charge separation and molecular oxygen activation, Angew. Chem. Int. Ed. 56 (2017) 11860–11864, https://doi.org/10.1002/anie.201706549.